PNAS RESEARCH ARTICLE | NEUROSCIENCE OPEN ACCESS

Lack of evidence for direct ligand-gated ion channel activity of GluD receptors

Masayuki Itoh[a,1], Laura Piot[b,1], Laetitia Mony[b], Pierre Paoletti[b,2], and Michisuke Yuzaki[a,2]

Affiliations are included on p. 6.

Edited by Richard Huganir, Johns Hopkins University School of Medicine, Baltimore, MD; received April 2, 2024; accepted May 10, 2024

Delta receptors (GluD1 and GluD2), members of the large ionotropic glutamate receptor (iGluR) family, play a central role in numerous neurodevelopmental and psychiatric disorders. The amino-terminal domain (ATD) of GluD orchestrates synapse formation and maturation processes through its interaction with the Cbln family of synaptic organizers and neurexin (Nrxn). The transsynaptic triad of Nrxn–Cbln–GluD also serves as a potent regulator of synaptic plasticity, at both excitatory and inhibitory synapses. Despite these recognized functions, there is still debate as to whether GluD functions as a "canonical" ion channel, similar to other iGluRs. A recent report proposes that the ATD of GluD2 imposes conformational constraints on channel activity; removal of this constraint by binding to Cbln1 and Nrxn, or removal of the ATD, reveals channel activity in GluD2 upon administration of glycine (Gly) and D-serine (D-Ser), two GluD ligands. We were able to reproduce currents when Gly or D-Ser was administered to clusters of heterologous human embryonic kidney 293 (HEK293) cells expressing Cbln1, GluD2 (or GluD1), and Nrxn. However, Gly or D-Ser, but also L-glutamate (L-Glu), evoked similar currents in naive (i.e., untransfected) HEK293 cells and in GluD2-null Purkinje neurons. Furthermore, no current was detected in isolated HEK293 cells expressing GluD2 lacking the ATD upon administration of Gly. Taken together, these results cast doubt on the previously proposed hypothesis that extracellular ligands directly gate wild-type GluD channels.

glutamate receptor | synapse | ion channel | glycine | D-serine

Significance

Delta receptors (GluD1 and GluD2), members of the large ionotropic glutamate receptor family, play a central role in many neurodevelopmental and psychiatric disorders. GluD regulates synapse formation and maturation by forming a transsynaptic tripartite complex with Cbln, a secreted synaptogenic molecule, and neurexin (Nrxn), independently of its ion channel activity. Recently, it has been reported that GluD2 could function as an ion channel that responds to D-serine (D-ser) and glycine (Gly) only when it forms a Nrxn/Cbln/GluD2 complex. Here, Itoh et al. provide evidence that GluD is not directly involved as an ion channel in the currents evoked by D-ser and Gly in heterologous cells and neurons. This finding is an important contribution to the ongoing discussion of the function of GluD.

Fast excitatory neurotransmission in the mammalian central nervous system is mediated by ionotropic glutamate receptors (iGluRs), which are classified into three types: α-amino-3-hydroxy-5-methyl-4-isoxazolepropionic acid (AMPA), kainate (KA), and N-methyl-D-aspartate (NMDA) receptors, each of which is activated by specific ligands. The delta receptors (GluD1 and GluD2), identified by homology screening (1, 2), constitute the fourth iGluR type but have long been considered orphan receptors. While GluD1 exhibits widespread expression throughout the brain, GluD2 is primarily found in the cerebellum (3–5). Mutations in these genes have been implicated in various neuropsychiatric and neurological disorders, such as schizophrenia and cerebellar ataxia, highlighting the importance of dissecting the GluD signaling pathway (6, 7). An important unresolved question is whether GluD functions as an ion channel or not. The ligand binding domain (LBD) of GluD, which shares a similar structural architecture with other iGluRs, undergoes conformational changes upon D-serine (D-Ser) and glycine (Gly) binding (8–11). However, D-Ser or Gly fail to evoke currents in human embryonic kidney 293 (HEK293) cells expressing GluD2 (10). Interestingly, the amino acid sequence near the end of transmembrane domain 3 (TM3), which serves as the channel gate in other iGluRs (6), is completely conserved in GluD. Introduction of a single amino acid mutation, the "*Lurcher*" mutation (GluD2^{Lc}), in this sequence renders GluD2 channels constitutively open without ligand binding (12, 13). Similarly, mutations in the TM3 region of GluD1 result in constitutively active GluD1^{Lc} channels (11, 14, 15). These constitutive GluD^{Lc} currents are modulated by D-Ser (or Gly) application and inhibited by the open channel blockers 1-naphthyl acetyl spermine (NASPM) and pentamidine (10, 11, 14–16). Furthermore, when the LBD of GluD was replaced by that of other iGluRs, GluD channel currents were elicited by glutamate application and inhibited by NASPM (17, 18). These results suggest that GluD can function as a channel when appropriate receptor alterations are introduced.

Interestingly, when GluD1 and GluD2 are coexpressed with metabotropic glutamate receptors (mGlu)1 or 5 in HEK293 cells, a slow inward current is observed upon administration of the mGlu1/5 agonist DHPG, which is suppressed by D-Ser or NASPM (19–21).

Author contributions: M.I., L.P., L.M., P.P., and M.Y. designed research; M.I. and L.P. performed research; M.I., L.P., L.M., P.P., and M.Y. analyzed data; and M.I., L.P., P.P., and M.Y. wrote the paper.

The authors declare no competing interest.

This article is a PNAS Direct Submission.

[1]M.I. and L.P. contributed equally to this work.

[2]To whom correspondence may be addressed. Email: pierre.paoletti@ens.psl.eu or myuzaki@keio.jp.

This article contains supporting information online at https://www.pnas.org/lookup/suppl/doi:10.1073/pnas.2406655121/-/DCSupplemental.

Published July 25, 2024.

Furthermore, mGlu-dependent inward current was suppressed by light in HEK293 cells coexpressing mGlu1 and an engineered GluD2 mutant allowing occlusion of the channel pore upon exposure to light (22). Similar mGlu-dependent slow inward currents are observed in GluD1-expressing dopaminergic neurons in the ventral tegmental area (20) and in GluD2-expressing cerebellar Purkinje cells (19, 21). In dorsal raphe neurons expressing α1-adrenergic receptors (α1-AR), GluD1 is required for inward currents induced by norepinephrine administration (23). These findings support the hypothesis that GluD acts as an ion channel when coexpressed with mGlu or α1-AR (24, 25), but the extent to which GluD directly contributes to the observed inward currents is not fully understood.

The amino-terminal domain (ATD) of GluD1 and GluD2 binds to Cbln2 and Cbln1, forming a tripartite complex with presynaptic neurexin (Nrxn) in Purkinje cells (26–28) and

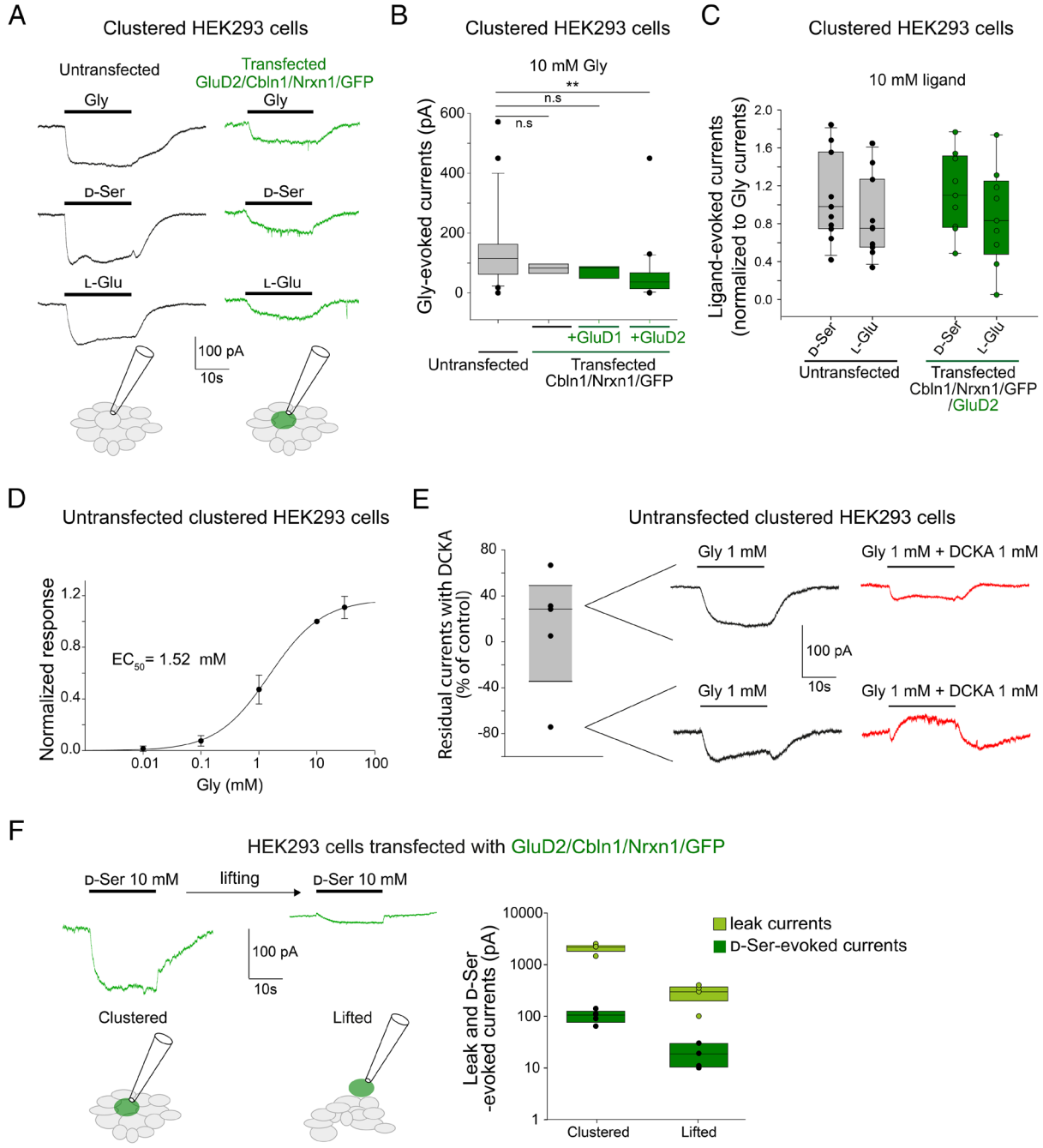

Fig. 1. Amino acids evoke currents in clustered naive (untransfected) HEK293 cells. (*A*) Gly, D-Ser and L-Glu (each at 10 mM) elicit robust inward currents in patch-clamped clustered HEK293 cells either untransfected (gray) or transfected (GluD2, Cbln1, Nrxn1, and GFP; green). (*B*) Amplitudes of Gly-evoked currents in clustered HEK 293 cells: untransfected (n = 22, gray), transfected with GFP, Cbln1, and Nrxn1 (n = 6, gray; $P = 1.0$), transfected with GFP, Cbln1, Nrxn1, and GluD1 (n = 7, green; $P = 0.705$), transfected with GFP, Cbln1, Nrxn1, and GluD2 (n = 19, green). No differences were found among four groups ($P = 0.00375$, Kruskal–Wallis with Dunn post hoc test with Bonferroni adjustment). (*C*) Comparison of D-Ser- and L-Glu-elicited currents normalized to Gly-evoked currents in clustered HEK293 cells: untransfected (gray; D-Ser n = 13 and L-Glu n = 14) and transfected with GFP, Cbln1, Nrxn1, and GluD2 (green; D-Ser n = 9 and L-Glu n = 9). No differences were found among four groups ($P = 0.638$, Kruskal–Wallis). (*D*) Dose–response curve of Gly-evoked currents in untransfected clustered HEK293 cells. (*E*) DCKA inhibits Gly-evoked currents in untransfected clustered HEK293 cells. Current traces on the *Right* corresponds to a single point on the *Left*. (*F*) Currents elicited by D-Ser in clustered (*Left*) or lifted (*Right*) configuration. *Right* panel: Amplitude of D-Ser-evoked (dark green) and leak (light green) currents in GluD2/Cbln1/Nrxn1/GFP transfected HEK293 cells in clustered or lifted configuration. n = 5; $P = 0.0079$ (two-sided Mann–Whitney test for both leak and D-Ser-evoked currents). Data are expressed as mean ± SD.

hippocampal neurons (29, 30), respectively. Recently, the ATD of GluD2 has been reported to repress the channel activity of GluD2, and this repression is lifted when the ATD forms a tripartite complex with Nrxn via Cbln1 (31). Under these conditions, GluD2 channel currents were observed upon administration of D-Ser or Gly. Given the paramount importance of this finding for understanding GluD channel function, we sought to validate the results of this work.

Results and Discussion

Constraining the conformation of ATD has been proposed to allow GluD2 to function as an agonist-gated ion channel (31). To test this hypothesis, and replicating the procedures described by ref. 31, we expressed GluD2 or GluD1 together with Cbln1 and Nrxn1 in HEK293 cell clusters. Application of Gly or D-Ser (10 mM each) induced inward currents (Fig. 1 *A* and *B*) in whole-cell voltage-clamped HEK293 cells, a result consistent with the previous report (31). However, L-glutamate (L-Glu) (10 mM), which does not bind GluD2 (10, 11), activated currents of similar amplitudes in cells coexpressing GluD2/Cbln1/Nrxn1 (Fig. 1 *A* and *C*). Remarkably, application of Gly (10 mM) elicited currents of similar amplitude in naive, i.e., untransfected, HEK293 cells, as well as HEK293 cells expressing only Cbln1/Nrxn1 (Fig. 1*B*). Application of D-Ser or L-Glu also induced inward currents of similar amplitudes in naive HEK293 cells and cells expressing Cbln1/Nrxn1/GluD2 (Fig. 1*C*). Similarly to Gly-evoked GluD2 currents reported in ref. 31, Gly-evoked currents in untransfected HEK293 cells displayed an EC_{50} of ~1.5 mM (Fig. 1*D*) and were inhibited by 5,7-Dichlorokynurenic acid (DCKA, 1 mM), an antagonist for the Gly site of NMDA receptors (32) and $GluD2^{Lc}$ currents (31, 33) (Fig. 1*E*). However, while constitutive $GluD^{Lc}$ currents are inhibited by NASPM (10, 12), an open channel blocker of Ca^{2+}-permeable AMPA and KA receptors (34), Gly-evoked currents observed in clustered naive HEK293 cells, as well as in cells expressing Cbln1/Nrxn1/GluD2, were insensitive to NASPM (*SI Appendix*, Fig. S1). Interestingly, currents induced by D-Ser (10 mM) were greatly reduced when the recorded HEK293 cells were isolated by lifting (Fig. 1*F*). Taken together, these results suggest that Gly and D-Ser, as well as L-Glu, when applied at high (mM) concentrations can activate large endogenous currents unrelated to GluD channels in naive HEK293 cell clusters.

To test GluD2 function independent of cell–cell contact, we next examined whether Gly could elicit currents in isolated and lifted HEK293 cells expressing GluD2 lacking the ATD (GluD2-ΔATD), in which the suppressive effects of the ATD on channel activity are absent (31). We used a piezoelectric element–based rapid perfusion system to minimize desensitization of channel currents (Fig. 2*A*). As a positive control, we used the flop isoform of the GluA2 AMPA receptor subunit, which carries glutamine (Q) at the channel pore [$GluA2^{flop}$(Q)]. As expected, application of L-Glu (3 mM) evoked rapidly desensitizing currents in HEK293 cells expressing $GluA2^{flop}$(Q) with a peak amplitude of ~1 nA (128.4 ± 17.37 pA/pF; Fig. 2 *B* and *E*). In contrast, although wild-type (WT) GluD2 and GluD2-ΔATD reached the cell surface (*SI Appendix*, Fig. S2), Gly (10 mM) failed to induce detectable currents in HEK293 cells expressing WT GluD2 (Fig. 2*C*) as well as GluD2-ΔATD (Fig. 2*D*). Therefore, in our hands and in contradiction to the results obtained by ref. 31, GluD2 receptors lacking the ATD do not display direct ligand-induced ionotropic activity.

It is possible that different HEK293 substrains express different endogenous genes, such as GluD or Nrxn, explaining the discrepancy between our results. However, since two laboratories (KUSM and IBENS) using HEK293 cells of different origin obtained essentially and independently the same results, this is unlikely (see Fig. 1 and *SI Appendix*, Fig. S1, whose data were obtained at IBENS and KUSM, respectively). We further investigated whether GluD2-dependent Gly currents are observed in Purkinje cells in acute

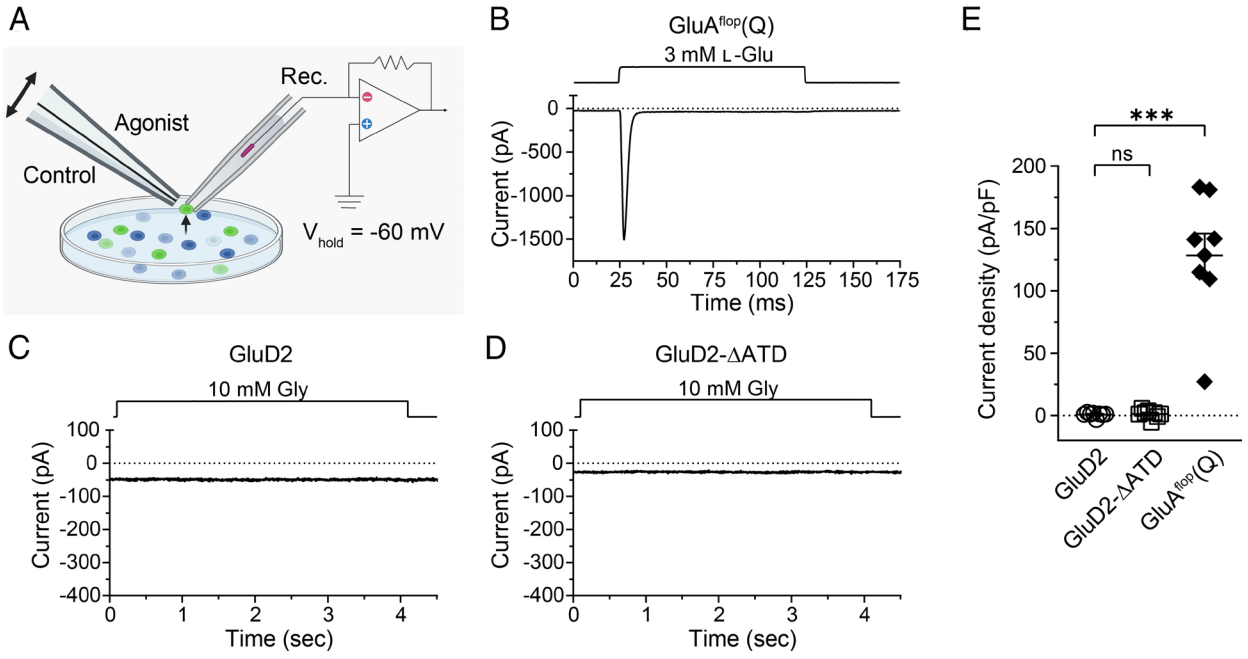

Fig. 2. Glycine does not induce currents in HEK293 cells expressing GluD2-ΔATD. (*A*) A schematic diagram illustrating the experimental setup. After whole-cell configuration, HEK293 cells were lifted and placed near the theta glass pipettes connected to the piezo element for rapid solution exchange. (*B-D*) Representative current traces of agonist-evoked currents recorded at a holding potential of −60 mV (lower traces). Liquid junction currents (upper traces) are shown to indicate the rate of solution exchange. Glu (3 mM)-evoked currents in cells expressing $GluA2^{flop}$(Q) (*B*), Gly (10 mM)-evoked currents in cells expressing WT GluD2 (*C*) and GluD2-ΔATD (*D*). (*E*) Plots summarizing the results. Current amplitudes were normalized to cell capacitance and plotted. Bars represent mean ± SEM (n = 8 each). $P > 0.999$ (GluD2 vs. GluD2-DATD) and $P = 0.0004$ [GluD2 vs. $GluA2^{flop}$(Q)] by Kruskal–Wallis test followed by Dunn's test.

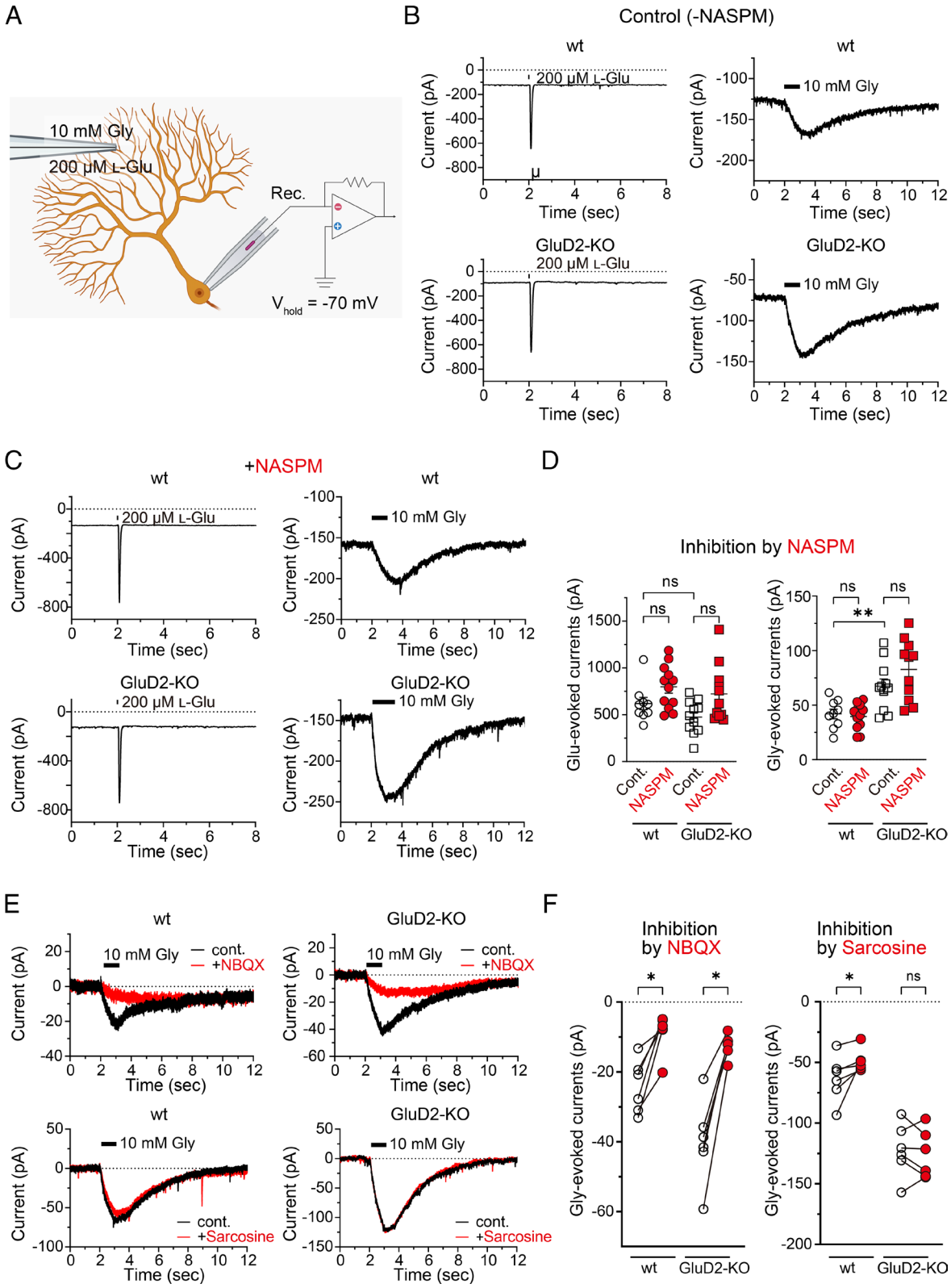

Fig. 3. Gly induces slow currents in Purkinje cells lacking GluD2 in acute slice preparations. (*A*) A schematic diagram illustrating the experimental setup. Responses of Purkinje cells voltage-clamped at −70 mV were elicited by local application of agonists through a theta-tube located in the molecular layer. (*B*) Representative current traces from Purkinje cells of WT (wt) and GluD2-null (KO) mice in response to 200 μM L-Glu or 10 mM Gly. (*C*) Representative recordings from Purkinje cells of wt and GluD2-KO mice in response to 200 μM L-Glu or 10 mM Gly in the presence of 100 μM NASPM. (*D*) Summarized plots showing the peak current amplitude elicited by the agonists. Bars represent mean ± SEM (n = 9 to 12 cells from at least two mice). For Glu-evoked currents, $P = 0.10$, 0.06, and 0.20 for wt vs. wt (+NASPM), GluD2-KO vs. GluD2-KO (+NASPM), and wt vs. GluD2-KO, respectively. For Gly-evoked currents, $P = 0.81$, 0.24, and 0.0097 for wt vs. wt (+NASPM), GluD2-KO vs. GluD2-KO (+NASPM), and wt vs. GluD2-KO, respectively. Mann–Whitney *U* test. (*E*) Representative current traces from Purkinje cells of WT and GluD2-null mice in response to 10 mM Gly with or without 50 μM NBQX (top traces) and 50 μM sarcosine (bottom traces). (*F*) Plots showing % inhibition before and after NBQX (*Left*) and sarcosine (*Right*) application. Bars represent mean ± SEM (n = 6 cells each). NBQX significantly inhibited Gly-evoked currents in wt ($P = 0.03$) and GluD2-KO ($P = 0.03$) Purkinje cells. Sarcosine inhibited Gly-evoked currents in wt ($P = 0.03$) but not in GluD2-KO ($P = 0.31$) Purkinje cells. Wilcoxon signed-rank test.

mouse cerebellar slices rather than in heterologous cells. Endogenous GluD2 is highly expressed in Purkinje cells and Cbln1 released from granule cells stabilizes GluD2 by simultaneously binding to its ATD and presynaptic Nrxn1 (26–28). L-Glu (200 μM) and Gly (10 mM) were locally applied to the dendrite of voltage-clamped Purkinje cells through the theta glass capillary connected to a pressure source (Fig. 3*A*). After adjusting the position of the theta-tube by observing L-Glu-induced currents, the pressure source was switched to the Gly side to record Gly-evoked currents. Upon L-Glu application, large inward currents that rapidly desensitized were similarly observed in WT and GluD2-null Purkinje cells (Fig. 3 *B* and *D*). These currents were insensitive to NASPM (Fig. 3*C*) but were largely inhibited by NBQX (*SI Appendix*, Fig. S3), a competitive antagonist for AMPA/KA receptors. Similarly, a slowly activating and recovering current was observed in both WT and GluD2-null Purkinje cells upon Gly application (Fig. 3 *B* and *D*). These Gly-induced currents were slightly larger in GluD2-null than WT Purkinje cells, yet of much smaller amplitudes than the L-Glu-induced currents. Gly-evoked currents were also largely insensitive to NASPM (Fig. 3 *C* and *D*), but were significantly inhibited by NBQX in both WT and GluD2-null Purkinje cells (Fig. 3 *E* and *F*), indicating that they are mediated, at least in part, by Ca^{2+}-impermeable AMPA/KA receptors. Sarcosine, a canonical inhibitor of the glial Gly transporter GlyT1 (35), only slightly reduced Gly-evoked currents in WT cells but not in GluD2-null Purkinje cells (Fig. 3 *E* and *F*). Although the precise mechanisms underlying Gly-evoked currents remain to be determined, these results indicate that GluD2 is unlikely to be a responsible channel since the current was observed in GluD2-null Purkinje cells and was insensitive to NASPM.

In this study, we reproduced the previous report (31) that Gly and D-Ser induced excitatory currents in HEK293 cells expressing Cbln1, Nrxn1, and GluD2 (or GluD1) in a cell–cell contact-dependent manner. However, Gly and D-Ser-evoked similar currents in untransfected HEK293 cells and Purkinje cells that do not express GluD2, indicating that these currents are unrelated to GluD1/2 channel activities. HEK293 cells endogenously express electrogenic amino acid transporters (e.g., refs. 36 and 37). Moreover, clustered HEK293 cells are connected extensively through gap junctions, thus displaying coupled electrical activity (e.g., ref. 38). We therefore propose that application of high concentrations (mM) of Gly, D-Ser, or L-Glu to HEK293 cells activates endogenous transporter currents, which when summed across a large number of cells (as recorded in HEK293 cell clusters), result in substantial overall currents (up to hundreds of pA). Our observation that L-Glu elicits currents of similar amplitudes to Gly or D-Ser-evoked currents further substantiates the disconnection with GluD, which is insensitive to L-Glu (10, 11). We also note that the currents recorded by Carrillo et al. are not inhibited by pentamidine, a classic channel blocker of most iGluRs including $GluD^{Lc}$ channels (11, 15, 39), again pointing to currents unrelated to GluD. Furthermore, rapid application of Gly failed to induce any currents in HEK293 cells expressing GluD2-ΔATD, in which the conformational constraints imposed by ATD are removed. Gly-evoked currents in Purkinje cells were likely mediated largely by Ca^{2+}-impermeable AMPA/KA receptors that were sensitive to NBQX but not NASPM (34). If cerebellar slices contain cells that express sarcosine-insensitive neuronal GlyT2 transporters (40), excitatory GlyRs (41), or metabotropic GlyRs (42), they would depolarize and potentially release L-Glu upon the application of Gly. This could lead to indirect activation of AMPA/KA receptors in Purkinje cells. The reasons for the discrepant results between our study and the one of (31) are unclear. However, it should be noted that in our hands, clearly defined currents are induced in naive HEK293 and GluD2-null Purkinje cells by application of Gly and D-Ser. Based on these findings, we do not support the assertion that Gly or D-Ser directly gates WT GluD channels.

GluD2 with a pore-occluding mutation in the channel (43) or composed only of ATD, transmembrane domain 4, and the C-terminal domain (CTD) (44) can restore synapse formation and synaptic plasticity in GluD2-null cerebellum. Similarly, in subiculum pyramidal neurons, GluD1 consisting only of ATD and CTD is sufficient to regulate postsynaptic AMPA and NMDA receptors (29). GluD1 also regulates the localization of postsynaptic GABA receptors in the cerebral cortex (45, 46) and the inhibitory synaptic plasticity in the hippocampus (11) even when GluD1 channels are rendered nonconductive. These results indicate that the extracellular domains and the CTD, but not the channel pore, are required for these functions of GluD1 and GluD2. Further studies are warranted to elucidate the molecular components of GluD-containing synapses to understand whether and how GluD exert ionotropic functions in specific cellular and synaptic contexts.

Materials and Methods

Electrophysiology in the Heterologous Expression System.

Yuzaki lab. The complementary DNA (cDNA) encoding mouse GluD2, GluD2-ΔATD, or rat $GluA2^{flop}$ (Q) was subcloned into the pTracer-EGFP vector (Thermo Fisher Scientific, Waltham, MA) as previously described (12). GluD2-ΔATD, which lacks the ATD (amino acids 24 to 439) (26), was produced by a PCR-based method. For surface immunostaining, a hemagglutinin (HA) tag with a liker sequence (GSA: glycine-serine-alanine) was inserted immediately following the signal peptide sequence of each construct.

HEK293 tSA cells (kindly provided by R. Horn, Thomas Jefferson Univ. Med. Sch., Philadelphia, PA; KUSM) were cultured in Dulbecco's modified Eagle's medium (DMEM) supplemented with 10% fetal bovine serum (FBS), 100 U/mL penicillin G, and 0.1 mg/mL streptomycin. For transient expression, cells were transfected with Lipofectamine 3000 (Thermo Fisher Scientific) according to the manufacturer's instructions. Before recording, the cells were detached from the culture dish and replated on glass coverslips.

Whole-cell voltage-clamp recordings were performed 24 to 48 h after transfection at room temperature. The extracellular solution contained (in mM) 145 NaCl, 5 KCl, 2 $CaCl_2$, 1 $MgCl_2$, 10 HEPES, and 10 glucose, pH adjusted to 7.4 with NaOH. The pipette solution contained (in mM): 147.5 CsCl, 1 $MgCl_2$, 4 Mg-adenosine triphosphate (ATP), 0.3 Na-guanosine triphosphate (GTP), 5 Cs_2EGTA, 0.1 spermine, and 10 2-[4-(2-hydroxyethyl)piperazin-1-yl] ethanesulfonic acid (HEPES), pH adjusted to 7.2 with CsOH, and the resistance of the patch pipette was 3 to 5 MΩ. Membrane currents recorded at a holding potential of −60 mV were low-pass filtered at 5 kHz and digitized at 50 kHz using an Axopatch 200B amplifier and Digidata 1550 controlled by pClamp 10.6 (Molecular Devices, San Jose, CA). To minimize rapid desensitization of iGluRs, agonist-containing solutions were perfused through a θ-shaped glass tube (tip diameter, 250 μm) controlled by a piezoelectric translator (LSS-3100, Burleigh Instruments, Fishers, NY) as previously described (12). This system typically allowed rapid solution exchange within 500 μs (20 to 80% rise time), as determined by measuring open-tip liquid junction currents at the end of each recording.

Paoletti lab. The cDNAs of the following genes were used: mouse *grid1* (GenBank 14803) in pcDNA3 for GluD1 with an HA tag inserted at the N terminus between amino acids 20 and 21 (20-TRYPYDVPDYA-21); mouse *grid2* (GenBank 14804) for GluD2 in pcDNA3; Nrxn1 as Nrx1bS4(+)S5(−)-3xFLAG in pCAGGS; Cbln1 as Myc-Cbln1 in pCAG; WT EGFP in pcDNA3.

HEK293 cells (obtained from ECACC) were cultured in DMEM containing 10% FBS and 1% Penicillin/streptomycin (5,000 U/mL). Transfections were performed using polyethylenimine (PEI) with a cDNA/PEI ratio of 1:3 (v/v), totalizing 1.0 μg DNA per well (24-well plate). Plasmid ratios were 1:1:1:0.25, when cotransfecting GluD, Nrxn, Cbln1, and EGFP, respectively. Patch-clamp recordings were performed 24 to 48 h following transfection. All recordings were performed in the whole-cell voltage-clamp configuration. The extracellular solution contained (in mM) 140 NaCl, 2.8 KCl, 1 $CaCl_2$, 10 HEPES, and 20 sucrose (290 to 300 mOsm), pH 7.3. The resistance of the patch pipettes was 3 to 7 MΩ, and the pipettes filled with an intracellular solution contained (in mM)

115 CsF, 10 CsCl, 10 HEPES, and 10 BAPTA (280 to 290 mOsm), pH 7.2. Currents recorded at a holding potential of −60 mV were sampled at 10 kHz and low-pass filtered at 2 kHz using an Axopatch 200B amplifier and Clampex 10.6 (Molecular Devices). Compounds were perfused on the patched cells using a multibarrel solution exchanger (RSC 200; BioLogic). All experiments were performed at room temperature.

Salts, L-Glu, Gly, D-Ser, and pentamidine were purchased from Sigma-Aldrich (St. Louis, MO, USA). DCKA was purchased from Tocris. DMEM (high glucose, GlutaMAX Supplement, pyruvate, GIBO™ ref. 31966021), FBS (GIBCO™, ref. 10270106), and penicillin/streptomycin (5,000 U/mL, GIBCO™ ref. 15140122) were purchased from ThermoFischer Scientific. PEI (ref. 23966-1) was purchased from Polysciences Europe.

Ex Vivo Slice Electrophysiology. All experiments related to animal care and treatment were approved by the Animal Resource Committee of Keio University (09050-9) and performed according to its guidelines. WT C57BL/6 N mice (Japan SLC) and GluD2-null mice (26, 27) aged 4 to 7 wk were subjected to electrophysiology. Until the experiments, mice were housed in a standard animal cage with a 12:12 h light–dark cycle and food and water available ad libitum.

Mouse brain slices were prepared as previously described with minor modifications (47). Briefly, mice were anesthetized with isoflurane and brains were rapidly removed. Parasagittal cerebellar slices from the vermis (250 μm in thickness) were prepared using Vibratome VT1200 S (Leica Biosystems, Wetzlar, Germany) in the ice-cold cutting solution (in mM: 215 sucrose, 2.5 KCl, 1.25 NaH_2PO_4, 0.1 $CaCl_2$, 10 $MgSO_4$, 20 HEPES, 25 glucose, 2 Na-ascorbate, 2 thiourea, and 1 N-Acetyl-L-cysteine, pH 7.4 with NaOH). After sectioning, slices were allowed to recover for at least 1 h at room temperature in the maintenance solution (in mM: 110 NaCl, 2.5 KCl, 1.25 NaH_2PO_4, 30 $NaHCO_3$, 2 $CaCl_2$, 1 $MgSO_4$, 20 HEPES, 25 glucose, 0.5 Na-ascorbate, 0.5 thiourea, and 0.1 N-Acetyl-L-cysteine, pH 7.4 with NaOH). All solutions for slice electrophysiology were equilibrated with 95% O_2 and 5% CO_2.

Each slice was transferred to the recording chamber on an upright microscope with a 60× water immersion objective (BX51WI, Tokyo) and perfused (~2 mL/min) with bath solution containing the following (in mM): 125 NaCl, 2.5 KCl, 1.25 NaH_2PO_4, 2 $CaCl_2$, 1 $MgSO_4$ 25 $NaHCO_3$, and 10 glucose. Whole-cell patch-clamp recordings were made from visually identified cerebellar Purkinje cells at room temperature as previously described (48). Patch pipette resistance was 3 to 5 MΩ when filled with Cs^+-based intracellular solution containing the following (in mM): 130 Cs-gluconate, 8 NaCl, 1 $MgCl_2$, 0.25 Cs_2-EGTA, 4 Mg-ATP, 0.3 Na-GTP, 5 Na-phosphocreatine, 5 QX314-Cl, 0.1 spermine, and 10 HEPES, pH 7.2 with CsOH. Membrane currents recorded at a holding potential of −70 mV were low-pass filtered at 2 kHz and digitized at 10 kHz using an Axopatch 200B amplifier and Digidata 1440 controlled by pClamp 10.6 (Molecular Devices). Liquid junction potential and series resistance were left uncompensated. Series resistance was monitored frequently during recording and neurons with >25 MΩ and a large drift (20%) in series resistance were excluded from analysis.

For rapid agonist delivery, two compartments of the θ-shaped glass tube (tip diameter approximately 2.5 μm) were filled with bath solution containing L-Glu (200 μM) and Gly (10 mM), respectively, and placed in the molecular layer at ~100 μm from the pial surface. A pressure pulse (10 to 20 psi; 50 ms for L-Glu and 1 s for Gly) was applied to each compartment using a pressure application system (Toohey Spritzer, Toohey Company, Fairfield, NJ). Picrotoxin (100 μM; Merck, Darmstadt, Germany), strychnine (1 μM; Merck), and D-AP5 (50 μM; Cayman Chemical, Ann Arbor, MI) were always included in the bath solution to block $GABA_A$R-, GlyR- and NMDAR-mediated currents. Additional blockers were used at the following concentrations: NASPM (Cayman Chemical), 100 μM; NBQX (Tocris Bioscience, Bristol, UK), 50 μM; Sarcosine (Tokyo Chemical Industry, Tokyo, Japan), 50 μM.

Data Analysis. The number of samples (n) indicates the number of different cells recorded. *P*-values are reported in the figures according to the following asterisk symbols: $*P < 0.05$, $**P < 0.01$, $***P < 0.001$. *P* values less than 0.05 were considered statistically significant. ns for "not significant."

Yuzaki lab. Data analysis was performed using the following software: pClamp 10.6 (Molecular Devices), Microsoft Excel (Microsoft, Redmond, WA), and Prism (Graphpad Software, San Diego, CA).

Paoletti lab. Data analysis was performed using SigmaPlot 11.0 (Systat Software). Gly dose-response curve was fitted with the following Hill equation: $I = 1/(1 + (EC_{50}/[C])^n)$, where I is the mean relative current, [C] the Gly concentration, and n the Hill coefficient. EC_{50} and n were set as free parameters. Statistical analysis was performed using Python mannwhitneyu from scipy.stats, using method = "exact" or using stats.kruskal and posthoc_dunn with Bonferroni p_adjust.

Data, Materials, and Software Availability. The dataset has been deposited on Mendeley Data (49). All study data are included in the article and/or *SI Appendix*.

ACKNOWLEDGMENTS. This work was supported by JSPS KAKENHI (Grant number: 21K06788 to M.I., 20H05628 to M.Y.), JST CREST (Grant number: JPMJCR1854 to M.Y.), JST ERATO (JPMJER1802 to M.I.), Sorbonne University (fellowship to L.P.), Fondation pour la Recherche Médicale (FRM; fellowship #FDT202012010605 to L.P.), Agence Nationale de la Recherche (ANR-23-CE16-0010-03 project GlueD to P.P.), and the European Research Council (ERC Advanced Grant #693021 to P.P.). We thank Dr. P. H. Seeburg for rat $GluA2^{flop}$(Q) cDNA. We are also grateful to J. Motohashi for animal maintenance.

Author affiliations: [a]Department of Physiology, Keio University School of Medicine, Tokyo 160-8582, Japan; and [b]Institut de Biologie de l'Ecole Normale Supérieure, Ecole Normale Supérieure, Université Paris Sciences & Lettres, CNRS, INSERM, Paris F-75005, France

1. K. Araki *et al.*, Selective expression of the glutamate receptor channel δ2 subunit in cerebellar purkinje cells. *Biochem. Biophys. Res. Commun.* **197**, 1267–1276 (1993).
2. H. Lomeli *et al.*, The rat delta-1 and delta-2 subunits extend the excitatory amino acid receptor family. *FEBS Lett.* **315**, 318–322 (1993).
3. R. Hepp *et al.*, Glutamate receptors of the delta family are widely expressed in the adult brain. *Brain Struct. Funct.* **220**, 2797–2815 (2015).
4. K. Konno *et al.*, Enriched expression of GluD1 in higher brain regions and its involvement in parallel fiber-interneuron synapse formation in the cerebellum. *J. Neurosci.* **34**, 7412–7424 (2014).
5. C. Nakamoto *et al.*, Expression mapping, quantification, and complex formation of GluD1 and GluD2 glutamate receptors in adult mouse brain. *J. Comp. Neurol.* **528**, 1003–1027 (2020).
6. K. B. Hansen *et al.*, Structure, function, and pharmacology of glutamate receptor ion channels. *Pharmacol. Rev.* **73**, 1469–1658 (2021).
7. M. Yuzaki, A. R. Aricescu, A GluD coming-of-age story. *Trends Neurosci.* **40**, 138–150 (2017).
8. A. C. Chin, R. A. Yovanno, T. J. Wied, A. Gershman, A. Y. Lau, D-serine potently drives ligand-binding domain closure in the ionotropic glutamate receptor GluD2. *Structure* **28**, 1168–1178. e2 (2020).
9. M. Masternak *et al.*, Differences between the GluD1 and GluD2 receptors revealed by GluD1 X-ray crystallography, binding studies and molecular dynamics. *FEBS J.* **290**, 3781–3801 (2023).
10. P. Naur *et al.*, Ionotropic glutamate-like receptor δ2 binds D-serine and glycine. *Proc. Natl. Acad. Sci. U.S.A.* **104**, 14116–14121 (2007).
11. L. Piot *et al.*, GluD1 binds GABA and controls inhibitory plasticity. *Science* **382**, 1389–1394 (2023).
12. K. Kohda, Y. Wang, M. Yuzaki, Mutation of a glutamate receptor motif reveals its role in gating and delta2 receptor channel properties. *Nat. Neurosci.* **3**, 315–322 (2000).
13. L. P. Wollmuth *et al.*, The lurcher mutation identifies δ2 as an AMPA/kainate receptor-like channel that is potentiated by Ca^{2+}. *J. Neurosci.* **20**, 5973–5980 (2000).
14. J. P. Allen *et al.*, Clinical features, functional consequences, and rescue pharmacology of missense *GRID1* and *GRID2* human variants. *Hum. Mol. Genet.* **33**, 355–373 (2023), 10.1093/hmg/ddad188.
15. R. Yadav, R. Rimerman, M. A. Scofield, S. M. Dravid, Mutations in the transmembrane domain M3 generate spontaneously open orphan glutamate delta 1 receptor. *Brain Res.* **1382**, 1–8 (2011).
16. K. B. Hansen *et al.*, Modulation of the dimer interface at ionotropic glutamate-like receptor δ2 by D-serine and extracellular calcium. *J. Neurosci.* **29**, 907–917 (2009).
17. A. Orth, D. Tapken, M. Hollmann, The delta subfamily of glutamate receptors: Characterization of receptor chimeras and mutants. *Eur. J. Neurosci.* **37**, 1620–1630 (2013).
18. S. M. Schmid, S. Kott, C. Sager, T. Huelsken, M. Hollmann, The glutamate receptor subunit delta2 is capable of gating its intrinsic ion channel as revealed by ligand binding domain transplantation. *Proc. Natl. Acad. Sci. U.S.A.* **106**, 10320–10325 (2009).
19. V. Ady *et al.*, Type 1 metabotropic glutamate receptors (mGlu1) trigger the gating of Glu D2 delta glutamate receptors. *EMBO Rep.* **15**, 103–109 (2014).
20. N. Benamer *et al.*, GluD1, linked to schizophrenia, controls the burst firing of dopamine neurons. *Mol. Psychiatry* **23**, 691–700 (2018).
21. S. Dadak *et al.*, mGlu1 receptor canonical signaling pathway contributes to the opening of the orphan GluD2 receptor. *Neuropharmacology* **115**, 92–99 (2017).
22. D. Lemoine *et al.*, Probing the ionotropic activity of glutamate GluD2 receptor in HEK cells with genetically-engineered photopharmacology. *Elife* **9**, e59026 (2020).
23. S. C. Gantz, K. Moussawi, H. S. Hake, Delta glutamate receptor conductance drives excitation of mouse dorsal raphe neurons. *Elife* **9**, e56054 (2020).
24. J. A. Abbott, G. K. Popescu, Homecoming of the estranged GluD channels. *Trends Neurosci.* **45**, 499–501 (2022).
25. J. Kumar, G. K. Popescu, S. C. Gantz, GluD receptors are functional ion channels. *Biophys. J.* **122**, 2383–2395 (2023).
26. J. Elegheert *et al.*, Structural basis for integration of GluD receptors within synaptic organizer complexes. *Science* **353**, 295–299 (2016).
27. K. Matsuda *et al.*, Cbln1 is a ligand for an orphan glutamate receptor delta 2, a bidirectional synapse organizer. *Science* **328**, 363–368 (2010).

28. T. Uemura *et al.*, Trans-synaptic interaction of GluRdelta2 and Neurexin through Cbln1 mediates synapse formation in the cerebellum. *Cell* **141**, 1068–1079 (2010).
29. J. Dai, C. Patzke, K. Liakath-Ali, E. Seigneur, T. C. Südhof, GluD1 is a signal transduction device disguised as an ionotropic receptor. *Nature* **595**, 261–265 (2021).
30. W. Tao, J. Díaz-Alonso, N. Sheng, R. A. Nicoll, Postsynaptic δ1 glutamate receptor assembles and maintains hippocampal synapses via Cbln2 and neurexin. *Proc. Natl. Acad. Sci. U.S.A.* **115**, E5373–E5381 (2018).
31. E. Carrillo, C. U. Gonzalez, V. Berka, V. Jayaraman, Delta glutamate receptors are functional glycine- and D-serine–gated cation channels in situ. *Sci. Adv.* **7**, eabk2200 (2021).
32. D. McNamara *et al.*, 5,7-Dichlorokynurenic acid, a potent and selective competitive antagonist of the glycine site on NMDA receptors. *Neurosci. Lett.* **120**, 17–20 (1990).
33. A. S. Kristensen *et al.*, Pharmacology and structural analysis of ligand binding to the orthosteric site of glutamate-like GluD2 receptors. *Mol. Pharmacol.* **89**, 253–262 (2016).
34. M. Koike, M. Iino, S. Ozawa, Blocking effect of 1-naphthyl acetyl spermine on Ca2+-permeable AMPA receptors in cultured rat hippocampal neurons. *Neurosci. Res.* **29**, 27–36 (1997).
35. K. E. Smith, L. A. Borden, P. R. Hartig, T. Branchek, R. L. Weinshank, Cloning and expression of a glycine transporter reveal colocalization with NMDA receptors. *Neuron* **8**, 927–935 (1992).
36. J. Dunlop, Z. Lou, H. B. McIlvain, Steroid hormone-inducible expression of the GLT-1 subtype of high-affinity L-Glutamate transporter in human embryonic kidney cells. *Biochem. Biophys. Res. Commun.* **265**, 101–105 (1999).
37. H. Toki *et al.*, Enhancement of extracellular glutamate scavenge system in injured motoneurons. *J. Neurochem.* **71**, 913–919 (1998).
38. A. M. Del Re, J. J. Woodward, Inhibition of gap junction currents by the abused solvent toluene. *Drug Alcohol. Depend.* **78**, 221–224 (2005).
39. K. Williams, M. Dattilo, T. N. Sabado, K. Kashiwagi, K. Igarashi, Pharmacology of δ2 glutamate receptors: Effects of pentamidine and protons. *J. Pharmacol. Exp. Ther.* **305**, 740–748 (2003).
40. E. Núñez, R. Martínez-Maza, A. Geerlings, C. Aragón, B. López-Corcuera, Transmembrane domains 1 and 3 of the glycine transporter GLYT1 contain structural determinants of *N*[3-(4′-fluorophenyl)-3-(4′-phenylphenoxy)-propyl]sarcosine specificity. *Neuropharmacology* **49**, 922–934 (2005).
41. S. Bossi *et al.*, GluN3A excitatory glycine receptors control adult cortical and amygdalar circuits. *Neuron* **110**, 2438–2454.e8 (2022).
42. T. Laboute *et al.*, Orphan receptor GPR158 serves as a metabotropic glycine receptor: mGlyR. *Science* **379**, 1352–1358 (2023).
43. W. Kakegawa, K. Kohda, M. Yuzaki, The δ2 'ionotropic' glutamate receptor functions as a non-ionotropic receptor to control cerebellar synaptic plasticity. *J. Physiol.* **584**, 89–96 (2007).
44. T. Torashima *et al.*, Rescue of abnormal phenotypes in δ2 glutamate receptor–deficient mice by the extracellular N-terminal and intracellular C-terminal domains of the δ2 glutamate receptor. *Eur. J. Neurosci.* **30**, 355–365 (2009).
45. E. Favuzzi *et al.*, Distinct molecular programs regulate synapse specificity in cortical inhibitory circuits. *Science* **363**, 413–417 (2019).
46. M. Fossati *et al.*, Trans-synaptic signaling through the glutamate receptor delta-1 mediates inhibitory synapse formation in cortical pyramidal neurons. *Neuron* **104**, 1081–1094.e7 (2019).
47. J. T. Ting *et al.*, Preparation of acute brain slices using an optimized N-methyl-D-glucamine protective recovery method. *J. Vis. Exp.* **132**, e53825 (2018), 10.3791/53825.
48. S. Wakayama *et al.*, Chemical labelling for visualizing native AMPA receptors in live neurons. *Nat. Commun.* **8**, 14850 (2017).
49. M. Yuzaki, P. Paoletti, Raw dataset for PNAS (Itoh et al, 2024). Mendeley Data. http://doi.org/10.17632/ps6245rd59.2. Deposited 9 July 2024.